Maximum Loading Capability of Axial Flow Compressors

J K Schweitzer* and J E Garberoglio†
Pratt & Whitney Aircraft, West Palm Beach, Florida

A maximum loading prediction system for determining the design speed stall margin capability of axial flow compressors is presented The formulation of the primary correlations for this system is based on the analogy between a compressor cascade and a diffuser passage Semiempirical corrections are applied to relate the initial cascade derived maximum loading values to the real compressor environment The system was formulated on the basis of meanline parameters, such that it can be used to guide the selection of the primary compressor design variables early in the design phase Good agreement is demonstrated between the predicted and test stall margins for a wide range of single and multistage compressor geometries

Nomenclature

A = cross sectional flow area, in ^{2}
AR = blade aspect ratio
AS = passage aspect ratio
b = blade chord length, in
c = clearance, in
C_L = lift coefficient
C_p = static pressure rise coefficient
D = diameter, in
f = friction factor
h = blade height, in
L = diffuser length, in
L_I = ideal static pressure rise coefficient
M = Mach number
N = number of airfoils
P = pressure, psia
PR = pressure ratio
R = radius, in
R_e = Reynolds number
t = thickness, in
T = temperature, R
Z = total pressure loss coefficient
β = relative air angle degrees from tangential
γ = ratio of specific heats
δ^* = boundary layer displacement thickness, in
ϵ = equivalent sand grain surface roughness, in
η = static pressure rise efficiency
θ^* = camber, deg
τ = tangential blade gap, in
ϕ = diffuser divergence angle, deg
Ω = relative loading parameter

Subscripts

eq = equivalent
H = hub
hyd = hydraulic
R = relative
S = stall
T = tip
0 = stagnation
1 = inlet
2 = exit

Presented as Paper 83 1163 at the AIAA 19th Joint Propulsion Conference Seattle Wash June 27 29 1983; received Aug 12 1983; revision received Jan 26 1984

*Design Technology Specialist Engineering Division Member AIAA
†Senior Engineer Engineering Division

Introduction

DURING the design of new axial flow compressors, an early estimate of the stall margin capability is a matter of great concern to the designer Insufficient stall margin at any point in the operating range can lead to serious problems in performance and/or durability; an overly conservative approach is usually accomplished only at the expense of an adverse tradeoff with compressor efficiency, number of stages, length, or weight While detailed refinements during development can lead toward attainment of a given compressor's full loading potential, in general, the level of this potential is determined once the primary design variables are selected during the preliminary design phase An accurate assessment of loading capability as early as possible in the design process, therefore, is essential.

Current compressor design practice has been to limit the loading in each compressor blade row through various loading parameters These have fallen into two general categories: airfoil aerodynamic loading parameters such as the diffusion factor and the equivalent diffusion ratio proposed by Lieblein et al ,[1,2] and endwall oriented loading parameters such as the blade row static pressure rise coefficient Previous attempts to correlate the maximum loading at stall based on these parameters have met with, at best, limited success While useful design criteria have resulted for similar compressor geometries, extrapolation outside the range of the data base upon which the correlations were formulated generally have proved inadequate Most recently Koch[3] pursued a diffuser analogy concept for correlating the maximum attainable loading at surge for compressor stages and showed that when the stage stalling static pressure rise coefficient was corrected to equivalent diffuser conditions, a trend with varying length to width ratio was obtained similar to that for two dimensional diffusers. Sufficient scatter was implied by the range of effective static pressure rise coefficient values calculated however, limiting its usefulness as a quantitative design tool

The objective of the analysis described herein was to develop an improved, more generally applicable system for predicting the maximum loading capability of axial flow compressors capable of guiding the selection of the primary compressor design variables early in the design phase This work was an extension of work originally initiated at Pratt & Whitney Aircraft (P&WA) in the late 1960's to formulate an equivalent conical diffuser correlation for axial compressor cascades,[4,5] and subsequently developed into a comprehensive meanline design system [6] The approach is similar to that of Koch in that it also is based on a diffuser analogy concept, except that the equivalent conical diffusion angle (representing the rate of diffusion) and the ideal loading,

which, in turn, is a function of the area ratio (amount of diffusion), are utilized as the primary correlating parameters The base correlations of the system were developed from an extensive series of in-house cascade tests with semiempirical corrections subsequently applied to relate the cascade correlation to any given compressor operating environment Diffuser and pipe flow data were employed where appropriate to help extrapolate the compressor and cascade derived correlations outside the range of available data A useful design tool has resulted which will be shown to exhibit good agreement between predicted and demonstrated compressor stall margin for a number of compressor geometries Further details of the system formulation and maximum loading analyses can be found in Ref 7

Diffuser Analogy

Since a compressor cascade is, in essence, a diffusing passage, it seems plausible that the same parameters that have been found to influence diffuser performance also could be used to correlate the performance of compressor cascades Straight wall two-dimensional and conical diffuser per formance has been shown by Dolan and Runstadler[8,9] and others to be a function of 1) geometric parameters including specification of both the area ratio, which establishes the overall amount of diffusion, and a normalized wall length, which establishes the rate of diffusion, and 2) the inlet flow parameters (Mach number, blockage, etc) For conical diffusers a third geometric variable, the diffuser included divergence angle (2ϕ), is also often employed Since the conical diffuser divergence angle can be expressed in terms of the area ratio (A_2/A_1) and passage length to inlet diameter ratio (L/D_1),

$$\tan\phi = \frac{\sqrt{A_2/A_1}-1}{2L/D} \tag{1}$$

specification of any two of those three variables characterizes the diffuser geometry sufficiently. Two-dimensional single-plane-divergence diffusers require an additional parameter, the passage aspect ratio, for their complete description and extension of the above to include curved diffusers further requires specification of the passage curvature.

In the present investigation, the compressor cascade is expressed in terms of an equivalent conical diffuser of the same area ratio and length as the cascade The primary geometric correlating parameters used are the equivalent conical diffusion angle (ϕ_{eq}) and the ideal loading (L_I), which for incompressible flow is a direct function of the area ratio

$$L_I = 1 - \left(\frac{1}{A_2/A_1}\right)^2 \tag{2}$$

Referring to Fig 1, equivalent conical section radii can be defined for the cascade inlet and exit,

$$R_{eq} = (A/\pi)^{1/2} \tag{3}$$

from which the equivalent diffusion angle ϕ_{eq} can be calculated:

$$\phi_{eq} = \tan^{-1}\left[\frac{R_{2eq}-R_{1eq}}{L}\right] \tag{4}$$

Rewriting this expression in terms of typical compressor cascade parameters and utilizing the blade chord as the representative length term, it can be shown that for a rec tangular cascade with no flow path convergence

$$\tan\phi_{eq} = \left[\frac{AR(\tau/b)}{\pi}\right]^{1/2}(\sin\beta_2^{\infty} - \sin\beta_1^{1/2}) \tag{5}$$

Since a compressor cascade is a turning passage and any given value of equivalent area ratio $(A_2/A_1) = f(\sin\beta_2/\sin\beta_1)$ can be attained over a range of inlet and exit flow angle combinations as the cascade stagger angle is varied, some correction for the amount of passage curvature is also required. For a typical circular arc camberline, the radius of curvature is inversely proportional to the difference between the inlet and exit angles In the current analysis, passage curvature effects, therefore, are accounted for by including the blade row turning $(\beta_2 - \beta_1)$ as one of the cascade correlation parameters

The need to account for the two dimensional characteristics of a compressor blade row through incorporation of the passage aspect ratio, given by $AS = AR/(\tau/b)\sin\beta$, while recognized, was not specifically included as a part of the initial cascade correlations since the passage aspect ratios of the cascade configurations tested were typically higher than the point below which passage aspect ratio effects become significant ($AS < 2\ 0$) Extrapolation of the cascade derived correlation to account for the effects of low passage aspect ratios is discussed in a later section

Maximum Loading Correlation

Cascade Data

Data used to derive the cascade maximum loading correlation came from two sources The first series of cascade data were taken in the Pratt & Whitney Aircraft suction tunnel and the second in the United Technologies Research Center (UTRC) cascade tunnel In all, a total of 121 cascade configurations was evaluated covering a wide range of design parameters

For the P&WA tunnel testing, the cascade span was kept constant at 11 in while the chord was varied between 2 and 4 in to yield a range of blade aspect ratios from 2 2 to 5 5 For each aspect ratio, gap to chord ratios of 0 817, 1 126, and 1.553 and stagger variations from 40 to 85 deg were evaluated All airfoil sections were circular arc sections with 30 deg of camber and a maximum thickness-to chord ratio of 0 0468 Each configuration was tested over a range of in cidence angles All data were acquired at an inlet Mach number of 0.25 with an inlet blockage of approximately 3% The tunnel endwalls were not bled

The UTRC tunnel configurations evaluated were run at a constant aspect ratio of 2 0 (4 in. span and 2 in chord) while the camber and thickness to chord ratio were varied from 10 to 50 deg and 5 to 9%, respectively The configurations were

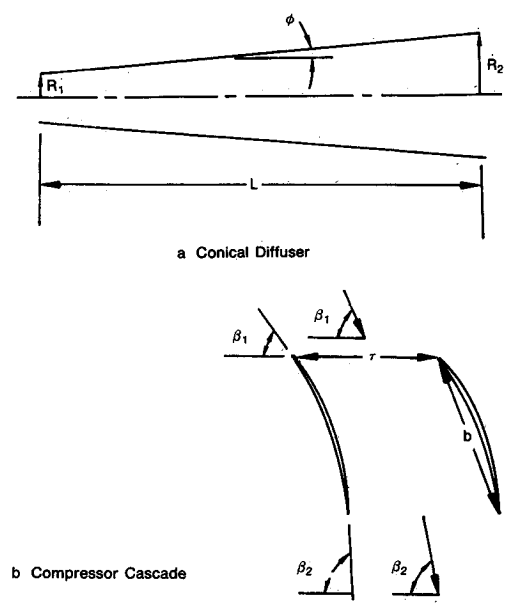

Fig. 1 Schematic of diffuser and cascade geometry

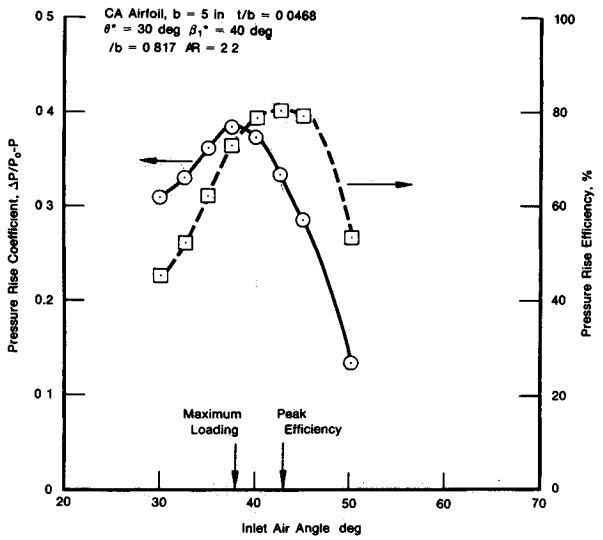

Fig. 2 Typical static pressure rise data from P&WA cascade tests

tested over a range of gap to chord ratios from 0 536 to 1 50 and a range of inlet air angles from 25 to 70 degs All data were acquired at an inlet Mach number of 0 4 As in the P&WA tunnel, the endwalls were not bled in the cascade passage and the inlet endwall boundary-layer thickness was estimated to give 3% blockage For each inlet air angle, the cascade stagger was varied to yield the desired range of incidence angles

The cascade performance from both tunnels was derived, similar to that of diffusers, in terms of the static pressure rise coefficient C_p and static pressure rise efficiency η, defined as:

$$\eta = C_p / C_{p_{\text{ideal}}} \tag{6}$$

A set of typical results is shown in Fig 2

Correlation Technique

Since the cascade configurations were run at various Reynolds numbers and sizes it was necessary to correct the data to standard values before correlating Each cascade configuration was corrected to a standard Reynolds number ($R_e = 10^6$), relative roughness ($\epsilon/D = 0\ 0008$), and effective entrance length ($b/D_{\text{hyd}} = 1$) This was accomplished through the use of the Moody diagram[10] to describe the relative change in the cascade friction factor and an entrance length effect as described by Ross [11] The static pressure rise efficiency η of each cascade was thereby corrected to the standard by ratioing the cascade inefficiency $(1-\eta)$ to the standard through the use of the ratio of the non fully developed friction factors derived from the Moody diagram and the Ross entrance effect In equation form this is:

$$(1-\eta)_{\text{corrected}} = (1-\eta)_{\text{uncorrected}} \left(\frac{f_{\text{standard}}}{f}\right)^{\ddagger} \left[\frac{(f/f_{\text{standard}})}{(f/f)}\right]^{\S} \tag{7}$$

Calculation of the friction factors used in the correction of the cascade pressure rise inefficiencies was made through the use of the Colebrook equation

$$1/\sqrt{f} = -2\log_{10}\left(\frac{\epsilon/D_{\text{hyd}}}{3.7} + \frac{2\ 51}{R_e\sqrt{f}}\right) \tag{8}$$

‡Factor derived from Moody diagram
§Factor derived from Ross entrance effect

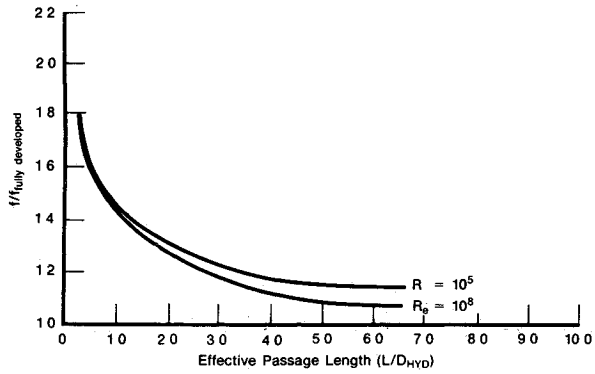

Fig 3 Loss due to passage length

as it represents the Moody diagram Use of this relationship required definition of the relative roughness of the airfoil and sidewall surfaces of the cascade The Moody diagram is based upon data taken from Nikuradse's experiments[12] in which he artificially roughened pipes by attaching graded size sand grain to the pipe surface. Nikuradse found the losses developed in the pipe to be directly a function of the relative roughness (ϵ/D) of the surface Later, experimenters discovered that these pressure losses are also a function of the relative spacing of the surface irregularities The sand grains in Nikuradse's experiments were quite closely spaced and, therefore, represented a "less" irregular surface than would be produced through normal manufacturing techniques Koch and Smith[13] subsequently showed the normal manufactured surface to be effectively 6 2 times as rough as that indicated by Nikuradse This relationship was adapted for the current investigation and can be expressed as

$$\epsilon = 6\ 2\epsilon_{\text{CLA}} \tag{9}$$

where ϵ_{CLA} is the centerline average surface roughness as measured by a profilometer

The Moody diagram, however, is based on fully developed flow Ross showed that in the entrance region of a pipe where the flow is not fully developed, the losses are considerably larger due to the development of the boundary layer on the walls The steeper velocity gradient in the cross span direction causes greater shear stresses and, therefore, greater frictional losses. The Moody diagram friction factors were, therefore, modified through a relationship derived by Ross to give the ratio of the loss in the entrance region to that loss that would occur in the same length of pipe for fully developed flow This relationship is shown graphically in Fig 3 An initial boundary layer at the entrance to the cascade reduces the shear stresses in the boundary layer and results in the effective length to diameter ratio of the cascade being larger than the actual cascade This effective length-to diameter ratio then is used to determine the above calculated loss ratio The relationship between the effective increase in inlet length and the inlet boundary layer thickness as a function of Reynolds number is shown in Fig 4

Correlation of the cascade maximum static pressure data was accomplished through the definition of a maximum loading quasiefficiency in which the maximum static pressure rise coefficient values were normalized by the ideal loading at the respective cascade peak efficiency points:

$$\eta_{\max} = \frac{[\Delta P/(P_0 - P)]_{\text{max demonstrated}}}{[\Delta P/P_0 - P]_{\text{ideal at peak efficiency}}} \tag{10}$$

The corrections applied to relate the cascade peak efficiency values to standard values of Reynolds number, relative roughness, and effective inlet length subsequently were ap

plied to the maximum loading quasiefficiencies and the resultant values correlated as a function of the cascade equivalent conical diffusion angle, ideal loading, and blade row turning at the peak efficiency point This technique of using correlation parameters and corrections defined at peak efficiency for correlating the maximum loading is employed for ease of eventual incorporation in the design process With this technique, definition of the cascade configuration at peak efficiency also results in definition of the maximum loading capability without the need for off-design calculations

Cascade Correlation

The corrected maximum pressure rise efficiencies for all of the cascade configurations evaluated are shown plotted against the respective equivalent conical diffusion angles in Fig 5. A consistent trend is evident in the data even though a wide range of ideal loading (0 07 0 63) and air turning angles (6 55 deg) are included in the cascade data base A regression analysis of this data to include these effects resulted in the following equation for the maximum pressure rise efficiency:

$$\eta_{\max} = -0\ 23355 + \frac{2\ 7847}{\phi^{1/2}} - \frac{2.0348}{\phi^{3/2}} + \frac{0.087858}{L_I} - 0\ 019203\Delta\beta^{1/2} \tag{11}$$

Multiplying through by the ideal loading yields the following direct expression for the maximum static pressure rise coefficient:

$$\left(\frac{\Delta P}{P_0 - P}\right)_{\max} = -0.23355L_I + \frac{2\ 7847L_I}{\phi^{1/2}} - \frac{2.0348L_I}{\phi^{3/2}} + 0\ 087858 - 0\ 019203\Delta\beta^{1/2}L_I \tag{12}$$

It should be noted that the correlation recognizes the effects of blading aspect ratio and solidity through the influence of these parameters on the equivalent cone angle.

The effect of blade row turning on the maximum pressure rise efficiency derived from the regression analysis is com pared in Fig 6 to circular arc diffuser data[14] obtained at two different area ratios The magnitude and general trend of the cascade derived correlation is seen to agree quite well with the diffuser data

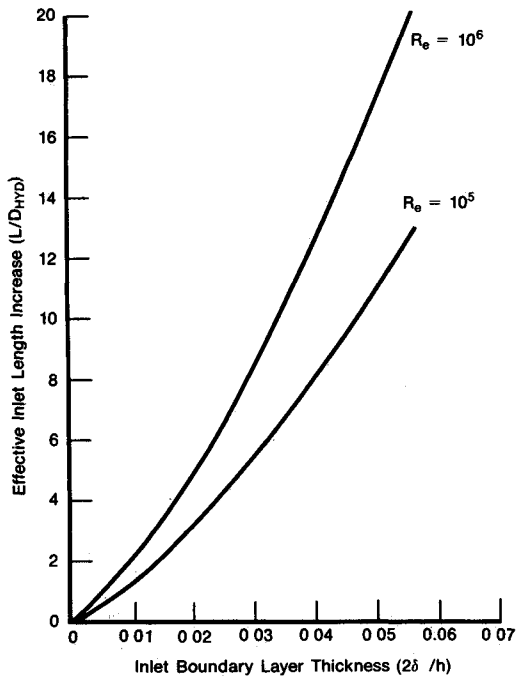

Fig 4 Effective increase in inlet length due to inlet boundary layer

Compressor Calculations

Since the data used in the derivation of the cascade correlation were referenced to a standard Reynolds number, relative roughness, and effective entrance length, application of the correlation to any given compressor blade row therefore requires appropriate adjustments to relate the cascade derived maximum loading values to the actual flow conditions These adjustments are applied in inverse fashion to the procedure outlined previously for initial correcting of the cascade data to the standard reference conditions In addition, the compressor blade row loading is influenced by several noncascade effects, including tip clearance and mean radius change through rotating blade rows, which need to be taken in account. Finally, small corrections also are required to account for nonstandard leading edge radii and passage aspect ratio effects outside the range of the cascade data base

These additional adjustments required to relate the cascade-derived maximum loadings to the actual compressor environment are described in the following paragraphs

Inlet Boundary-Layer Thickness

It is well known that the inlet boundary-layer thickness to a diffuser has a large effect on the pressure rise of the diffuser. Rundstadler and Dolan,[8,9] Ackeret,[15] and others, have documented this effect. Similarly, compressors are also highly responsive to the relative boundary layer on the endwall at the entrance to each blade row Since the cascade-derived maximum loading correlation was developed from data all taken with an inlet blockage of approximately 3%, some correction is required to account for the effects of varying inlet relative boundary-layer thicknesses.

Figure 7 shows P&WA results where cascade performance was found with different inlet boundary layers This data

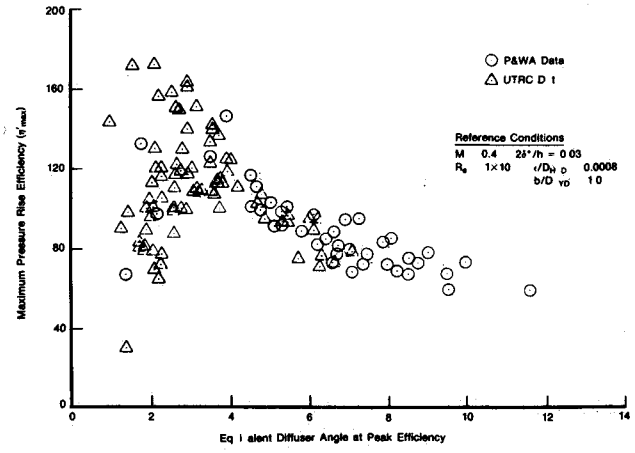

Fig 5 Cascade data correlation of maximum pressure rise efficiency

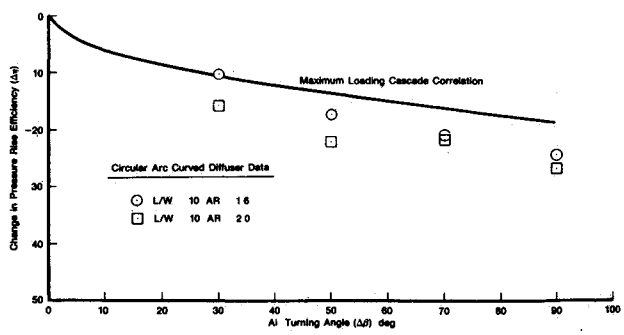

Fig 6 Effect of air turning on maximum loading capability

shows good agreement with the diffuser data and is described analytically by the relationship

$$\eta = 1/\left[C\left(\frac{2\delta^*}{h}\right) + 1\ 225\right]^{0\ 25} \tag{13}$$

where C is a slope coefficient given by

$$C = \left[\left(\frac{1}{\eta_{\text{at } 2\delta^*/h = 0\ 03}}\right)^4 - 1\ 225\right]/0\ 03 \tag{14}$$

Mach Number

Typical modern advanced compressors operate over a wide range of Mach numbers, including the high transonic and supersonic regimes. Corrections in the calculation of the ideal loading and equivalent conical diffusion angle are therefore required to account for compressibility effects. These are accomplished by using the area ratio from the equivalent incompressible diffuser that would be required to give the same velocity change as the actual compressor blade row Increasing the Mach number always gives a larger equivalent area ratio than the physical area ratio. The appropriately corrected expressions for the ideal loading and equivalent conical diffuser angle, respectively, are given by

$$L_I = \frac{(P/P_0)_2 - (P/P_0)_1}{1 - (P/P_0)_1} \tag{15}$$

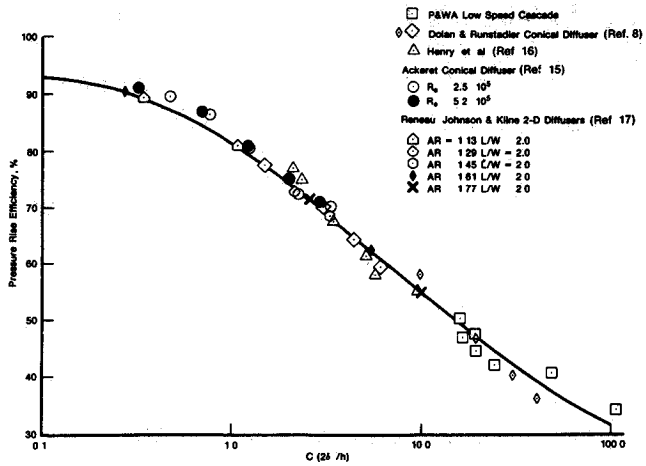

Fig. 7 Effect of inlet boundary-layer blockage

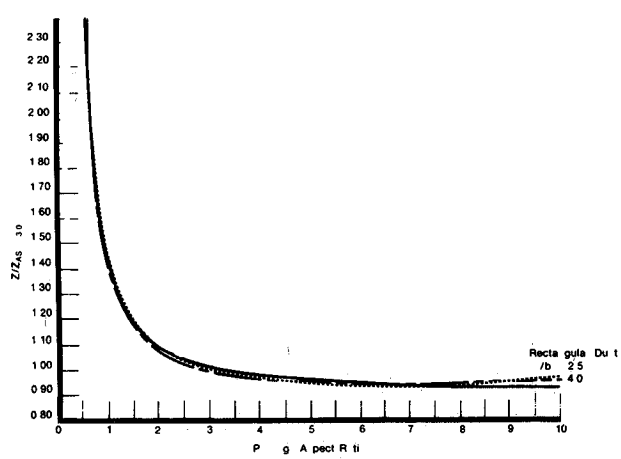

Fig 8 Effect of passage aspect ratio

$$\tan\phi_{eq} = \frac{[(D_{T1}^2 - D_{H1}^2)\sin\beta_1]^{1/2}}{2bN^{1/2}}\{(1-L_I)^{-0\ 25} - 1\} \tag{16}$$

Additional losses also occur as the blade row inlet relative Mach number approaches the transonic region and proceeds into the supersonic region These losses are due to the for mation of shocks and the interaction of these shocks with the blade row suction surface boundary layer In order to preclude use of design calculations, for the present analysis the Mach number related losses resulting from a design point meanline efficiency analysis are converted into a corresponding reduction in the blade row static pressure rise, which, in turn, is subtracted directly from the predicted in compressible maximum loading capability While further refinement to properly account for the changes in inlet relative flow conditions between the design and stall points may seem prudent, the present simplifying assumptions appear adequate for the current study

Tip Clearance

The loss in static pressure rise due to tip clearance is represented in the present analysis by the semiempirical model developed by Lakshminarayana.[18] The basic relationship derived from this model gives the loss as

$$\Delta C_p = \frac{0\ 7 C_L^2 (c/h)}{(\tau/b)^2 \sin\beta_m}\left[1 + 10\left(\frac{\tau}{b}\frac{c}{h}AR/C_L\right)^{1/2}\right] \tag{17}$$

Rotor Radius Change

The change in mean rotor speed associated with an increase in the mean radius through a rotating blade results in an increase in the relative enthalpy The increase in static pressure rise associated with this increased work is considered "free" (in addition to that which could be attained through a similar blade row with no radius change) since it does not require any diffusion of the relative velocity Starting with the well-known Euler work equation, the following expression for the change in static pressure rise capability due to mean rotor radius variations can be derived:

$$(\Delta P)_{\text{radius}} = P_{01R}\left\{\left[1 + \frac{(\gamma-1)(U_2^2 - U_1^2)}{2g\gamma R T_{01R}}\right]^{\gamma/(\gamma-1)} - 1\right\}\Big/ \left\{\left[1 + \frac{\gamma-1}{2}(M_{1R})^2\right]^{\gamma/(\gamma-1)}\right\} \tag{18}$$

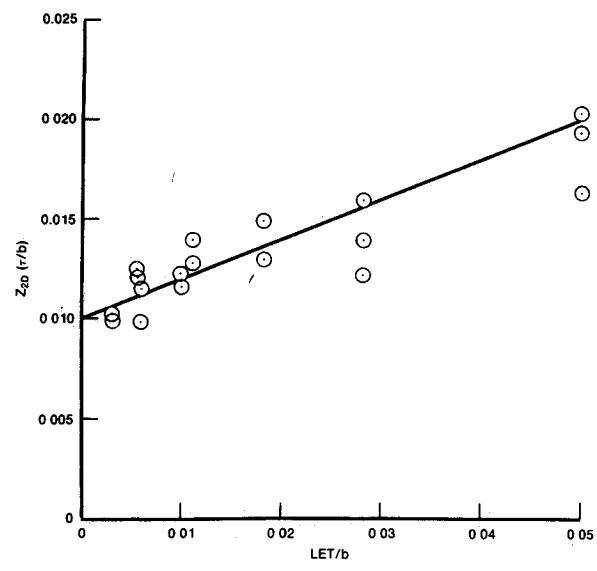

Fig 9 Profile minimum loss as a function of leading edge thickness

Passage Aspect Ratio

Passage aspect ratio is known to be an important parameter influencing diffuser performance Rundstadler[9] observed that for low inlet blockage flow in two dimensional diffusers, a predominant effect on pressure recovery occurs at low (<2 0) passage aspect ratio values Since the passage aspect ratios of the cascade configurations used to develop the maximum loading correlation generally were greater than 2 0, a comparable trend could not be delivered directly from the cascade data However, advanced low aspect ratio, highly loaded compressor blade rows can have passage aspect ratio values less than 2.0 Thus, some method of extrapolating the cascade correlation to lower passage aspect ratio values was required

The method used was formulated from rectangular duct loss data obtained from Ref 19 which includes the effect of passage aspect ratio on loss coefficient for the flow through 90-deg rectangular bends at various radius ratios Calculation of equivalent radius ratios for a number of compressor blade rows indicated the radius ratio to be characteristically between 2 5 and 4 0 Ratioing the Ref 19 loss values for radius ratios in the range 2 5 4 0 to the loss values at a passage aspect ratio of 3 0 and superimposing the results (Fig 8) shows a consistent variation in loss as a function of passage aspect ratio This trend generally agrees with Rundstadler's diffuser data and, when incorporated in the maximum loading system, provides consistent results for those compressors modeled to date with low passage aspect ratio blade rows

Leading Edge Bluntness

Variations in the leading edge thickness of compressor airfoils are known to influence the airfoil total pressure profile loss characteristics These profile loss variations can, in turn, be translated into a change in the airfoil maximum loading (static pressure rise) capability. Typical P&WA low speed cascade data for airfoils with circular leading edges are presented in Fig 9 showing the variations in minimum profile loss as a function of leading-edge thickness to-chord ratio The simpler linear relationship shown on the figure has been found to describe this effect adequately for the purposes of the present study

Stall Margin Correlation

The cascade maximum loading correlation, when appropriately corrected to the actual compressor operating environment as outlined in the previous section, provides an estimate of the maximum loading capability for each individual blade row of a given compressor The conversion of the collective individual blade row loadings into an overall compressor maximum loading prediction and the relationship of this maximum loading to the compressor stall margin potential from peak efficiency is discussed in the following

For each compressor blade row a relative loading parameter Ω, indicating the proximity of that blade row to its maximum loading capability, can be defined as

$$\Omega = \frac{\Delta P/P_0 - P}{(\Delta P/P_0 - P)_{\max}} \tag{19}$$

where $\Delta P/P_0 - P$ is the actual static pressure rise coefficient for that blade row at any given point and $(\Delta P/P_0 - P)_{\max}$ is the predicted maximum loading obtained from the correlation The distribution of the individual blade row relative loadings for a number of compressors was examined both at peak efficiency and near stall in order to evaluate the behavior of the relative loading parameter and identify the limiting stage (or stages) This examination indicated two factors which needed to be taken into account The first of these was the fact that at design speed the rear stages of a compressor tend to load up more rapidly than the front stages

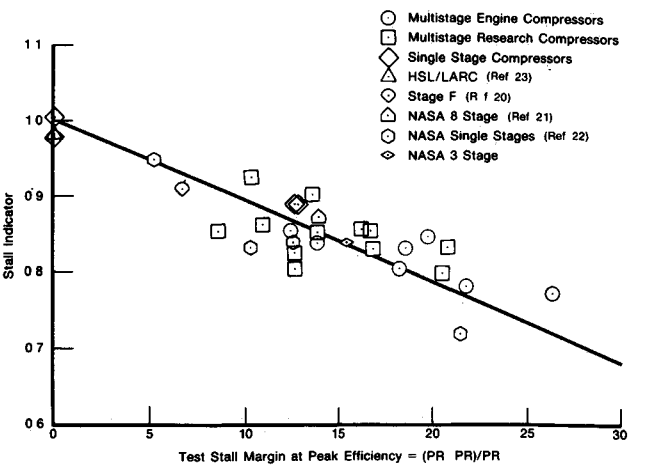

Fig 10 Compressor stall margin correlation

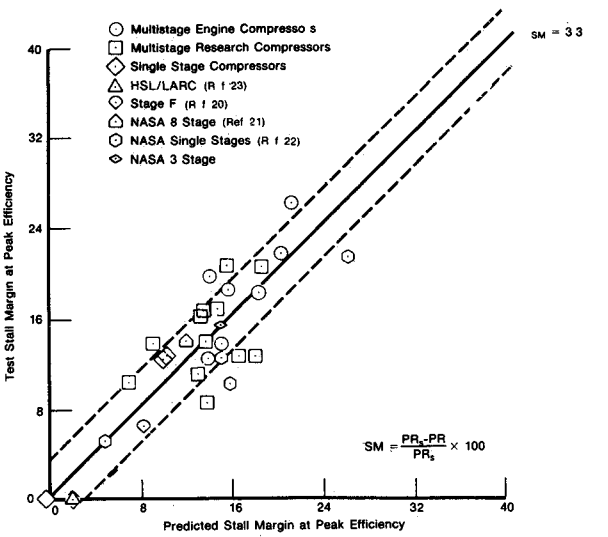

Fig 11 Stall margin correlation prediction accuracy

for a properly matched design as stall is approached Thus, even though a rear stage may be relatively more lightly loaded than a front stage at peak efficiency, the rear stage in many cases could be the stall limiting stage The second factor is the observation that lightly loaded upstream and downstream adjacent blade rows can have a significant stabilizing effect, such that individual blade row relative loading values greater than one can and often do exist within the overall compressor stable operating range

Some method of averaging the individual blade row relative loading levels thus was required in order to provide an indication of the overall compressor loading potential Accordingly, a stall indicator (SI) was formulated which provides a weighted average of the individual blade row relative loadings taking into account the two factors discussed above:

$$\mathrm{SI} = \frac{\bar{\Omega}}{2}\left[1 + \left(\frac{\Omega_p}{\bar{\Omega}}\right)^{PS/\mathrm{NOS}}\right]_{\max} \tag{20}$$

where $\bar{\Omega}$ is the average loading parameter of the entire compressor; Ω_p the rotor peak loading parameter; PS the stage number in which Ω_p occurred; and NOS the total number of stages

A measure of the degree of nonuniformity of the individual blade row relative loadings is included through the $\Omega_p/\bar{\Omega}$ term with the magnitude of the effect of this nonuniformity

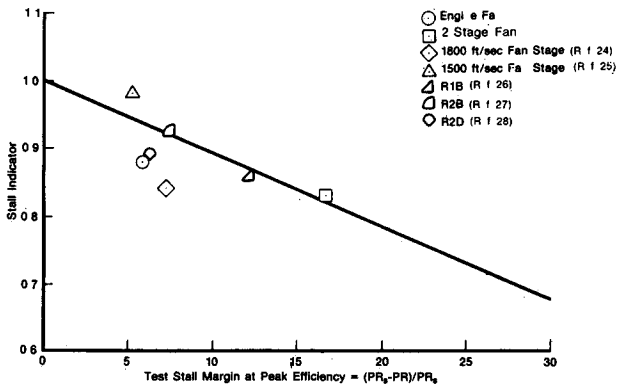

Fig. 12 Comparison of fan stall margins with compressor correlation

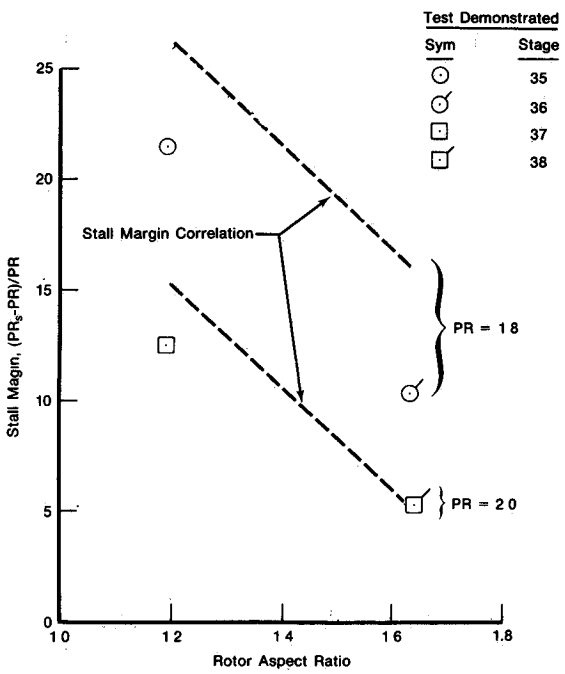

Fig 13 NASA single stages stall margin variation with aspect ratio

dependent on the stage number in which the peak relative loading occurs (through the exponent *PS*/NOS).

Figure 10 shows stall indicator values calculated at the design speed peak efficiency points plotted vs demonstrated stall margin for 31 high pressure compressor configurations Included in this data base are both single- and multistage compressors covering a wide range of design variables, in cluding compressors with both highly skewed and fairly uniform loading distributions A linear regression analysis was conducted to fit a line to the data with the following result:

$$\% \text{ stall margin} = 93\ 958\ (1\text{-SI}) \qquad (21)$$

A direct comparison of the test vs predicted stall margin for the same 31 compressor configurations is presented in Fig 11 A good match of the demonstrated stall margin is evident with a rms deviation of 3 3% stall margin for the collective data set

The maximum loading prediction system was formulated based on static pressure rise characteristics, hence, it was intended to be primarily applicable to endwall limited blade rows (as is typically the case for multistage high pressure compressor configurations). Since the hub to tip radius ratio for the Fig 10 compressors ranged from 0 5 to 0 9, the stall

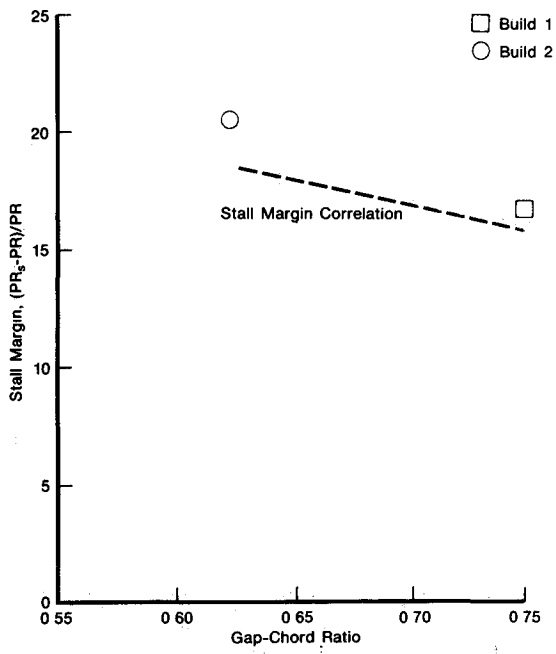

Fig 14 P&WA high speed rig stall margin variation with solidity

margin correlation was examined in an attempt to identify areas of potential blading diffusion, as opposed to endwall loading, limitations; however, no biases were apparent A number of fans and single stages with hub to tip radius ratios in the 0 3 0 5 range were subsequently analyzed and are compared to the compressor correlation in Fig 12 In general, the stall indicator trend, as a function of the demonstrated stall margin, agrees with that obtained for the compressor stages However, further analysis of low hub-to-tip radius ratio stages is recommended prior to utilization of the correlation for these potentially blading diffusion limited configurations

In order to obtain full benefit from usage of the maximum loading prediction system as a design tool, it was desired that the system be capable of predicting the effects of variations in the primary compressor design variables on the maximum loading capability To verify the effects of aspect ratio, four highly loaded NASA single stages[22] encompassing two levels of aspect ratio at each of two stage pressure ratios were analyzed The results (Fig. 13) show that the maximum loading system accurately predicts the relative change in stall margin with variation in aspect ratio at both pressure ratios although there is some bias in the level of the predicted stall margin at the lower pressure ratio Solidity effects are illustrated in Fig 14, where the predicted and demonstrated variation in stall margin is shown for a P&WA highly loaded three-stage research rig in which the number of airfoils was varied in subsequent tests Again, good agreement between the predicted and demonstrated stall margin is apparent

Conclusions

A maximum static pressure rise capability correlation was developed from low-speed cascade data utilizing the analogy between compressor cascade and a diffuser passage to define the primary correlating parameters Accounting for the ef fects of Reynolds number, inlet boundary layer blockage, surface finish, tip clearance, passage aspect ratio, leading edge bluntness, rotor radius change, and Mach number, it was shown that the cascade correlation could be related to a multistage environment An overall compressor stall index subsequently was formulated from the individual blade row relative loadings which was shown to vary in a linear fashion with the demonstrated stall margin for a number of single and multistage compressors The resulting formulation can be

used to estimate the stall margin potential within a rms accuracy of approximately 3 3% for any given compressor configuration The system is derived totally from meanline type information, hence, it is applicable during the initial compressor preliminary design phases

Acknowledgment

The work presented herein was conducted for the Air Force Wright Aeronautical Laboratories, Aero Propulsion Laboratory, under Contract F33615 76-C 2091.

References

[1]Lieblein, S Schwenk F D., and Broderick, R L , "Diffusion Factor for Estimating Losses and Limiting Blade Loadings in Axial Flow Compressor Blade Elements, NACA RM E53D01 June 1953

[2]Lieblein S , Loss and Stall Analysis of Compressor Cascades ' *ASME Journal of Basic Engineering* Vol 81 Sept 1959 pp 387 400

[3]Koch C C Stalling Pressure Rise Capability of Axial Flow Compressor Stages ' ASME Paper 81 GT 3 March 1981

[4]Edmonds S A Equivalent Conical Diffusion Angle Correlation for Axial Compressor Cascades ' P&WA Internal Memorandum Aug 14, 1969

[5]Edmonds, S A ' Compressor Cascade Maximum Loading Correlation, ' P&WA Internal Memorandum Dec 18 1975

[6]Edmonds S A and Jones, M G 'Equivalent Conical Diffusion Angle Analogy—Cascade Correlation and Meanline Program For mulation ' P&WA FTDM 571 Dec 31, 1975

[7]Schweitzer J K and Garberoglio, J E , Loading Capability of Axial Flow Compressor Systems, AFWAL TR 82-2041 June 1982

[8]Dolan, F. X and Rundstadler, P W Jr 'Pressure Recovery Performance of Conical Diffusers at High Subsonic Mach numbers NACA CR 2299 Aug 1973

[9]Rundstadler, P W Jr , ' Pressure Recovery Performance of Straight Channel; Single Plane Divergence Diffusers at High Mach Numbers USAAVLADS Tech Rept 69 56 Oct 1969

[10]Moody L F , Friction Factors for Pipe Flow *Transactions of the ASME* Nov 1944

[11]Ross D. "Turbulent Flow in the Entrance Region of a Pipe, ASME Paper 54 A 89, July 1956

[12]Nikuradse J Laws of Flow in Rough Pipes, NACA TM 1292 Nov 1950

[13]Koch C C and Smith L H Loss Sources and Magnitudes in Axial Flow Compressors *ASME Journal of Engineering for Power* Vol 98 July 1976, pp 411-424

[14]Sagi C J and Johnston J P Jr , The Design and Per formance of Two Dimensional Curved Diffusers, *ASME Journal of Basic Engineering*, Vol. 89 Dec 1967 pp 715 731

[15]Ackeret, J "Boundary Layers in Straight and Curved Dif fusers, ' *IUTAM Symposium on Boundary Layer Research* Springer-Verlag Berlin, FRG, 1958, pp 22-40

[16]Henry, J R , Wood C C and Wilbur S W., "Summary of Subsonic-Diffuser Data,' NACA RM L56F05 Oct. 1956.

[17]Reneau, L R , Johnston J P. and Kline, S J , "Performance and Design of Straight, Two-Dimensional Diffusers " AMSE Paper 66-FE-10, 1966.

[18]Lakshminarayana B. "Methods of Predicting the Tip Clearance Effects in Axial Flow Turbomachinery," *ASME Journal of Basic Engineering*, Vol 92, Sept. 1970 pp. 467 482.

[19]*SAE Aero-Space Applied Thermodynamics Manual*, 2nd Ed., Society of Automotive Engineers, Warrendale, Pa., 1969, pp. 3-28.

[20]Cheatham, J G , Smith J D and Wright, D L , Single Stage Experimental Evaluation of Low Aspect Ratio, Highly Loaded Blading for Compressors Part IX Final Report Stage F and Stage G NASA CR-134993, Vol 1 May 1976

[21]Geye R P Budinger, R E and Voit C H ' Investigation of a High Pressure Ratio Eight Stage Axial Flow Research Compressor with Two Transonic Inlet Stages Part II—Preliminary Analysis of Overall Performance ' NACA RM E53J06 Dec. 1953

[22]Reid, L and Moore R D Design and Overall Performance of Four Highly Loaded High Speed Inlet Stages for an Advanced High-Pressure Ratio Core Compressor, ' NASA TP 1337 Oct 1978

[23]Brent J A Cheatham, J G , and Singleton, E T High Stage Loading/Low Aspect Ratio Compressor (HSL/LARC) Final Report (U) ' AFWAL TR 80 2075, Vol 1 Sept 1980

[24]Morris A L and Sulam D H High Loading 1800 ft/sec Tip Speed Transonic Compressor Fan Stage Part II Final Report,' NASA CR 120991 Dec 1972

[25]Wennerstrom A J. Law, C H Buzzell W A , and De Rose, R D ' Investigation of a 1500 ft/sec Transonic High-Through Flow Single-Stage Axial Flow Compressor with Low Hub/Tip Ratio AFAPL TR 76-92, Oct 1976

[26]Seyler D R and Gostelow J P Single Stage Experimental Evaluation of High Mach Number Compressor Rotor Blading Part 2—Performance of Rotor 1B,' NASA CR 54582, Sept 1971

[27]Gostelow, J. P and Krabacher K W ' Single-Stage Ex perimental Evaluation of High Mach Number Compressor Rotor Blading Part 5—Performance of Rotor 2B,' NASA CR 54585 Oct 1967.

[28]Krabacher K W and Gostelow J. P Single Stage Experimental Evaluation of High Mach Number Compressor Rotor Blading Part 4—Performance of Rotor 2D NASA CR 54584 Oct 1967